Magnetic structure and critical behaviour of the Heisenberg limit triangular antiferromagnet $CsMn(Br_{0.19}I_{0.81})_3$

1999 J. Phys.: Condens. Matter 11 4427

(http://iopscience.iop.org/0953-8984/11/22/313)

J. Phys.: Condens. Matter **11** (1999) 4427–4433. Printed in the UK PII: S0953-8984(99)98892-6

Magnetic structure and critical behaviour of the Heisenberg limit triangular antiferromagnet $CsMn(Br_{0.19}I_{0.81})_3$

T Ono†, H Tanaka†, T Kato†, K Nakajima‡ and K Kakurai‡

† Department of Physics, Tokyo Institute of Technology, Oh-okayama, Meguro-ku, Tokyo 152-8551, Japan

‡ Neutron Scattering Laboratory, Institute for Solid State Physics, University of Tokyo, Tokai, Naka-gun, Ibaraki 319-1106, Japan

Received 2 November 1998, in final form 10 March 1999

Abstract. Elastic neutron scattering experiments were carried out to investigate the magnetic structure and the critical behaviour of the mixed triangular antiferromagnetic system $CsMn(Br_{0.19}I_{0.81})_3$, for which our previous magnetic measurement revealed the macroscopic anisotropy to be negligible. It is found that in the ordered state below $T_N = 8.29$ K, the spin planes in which the spins lie with the 120° structure are tilted from the basal plane, and that the average of the tilting angle ϕ is evaluated as $\langle\cos^2\phi\rangle = 0.362$, i.e. $\langle\phi\rangle = 53°$. This result suggests that the present system is almost at the Heisenberg limit for the interaction. The critical exponent for the sublattice magnetization is obtained as $\beta = 0.28 \pm 0.02$, which is in agreement with the value predicted for the chiral Heisenberg universality class.

1. Introduction

In stacked triangular antiferromagnets (TAF), the spin frustration produces a variety of phase transitions [1]. For the XY and Heisenberg spin systems, the 120° spin structure is realized in the ordered state. The noncollinearity of the spin structures leads to new degrees of freedom, 'chirality' [2, 3]. Due to the chirality, the critical behaviour of the TAF differs from those of the unfrustrated systems. Kawamura [4] argued that the stacked XY and Heisenberg TAFs belong to the chiral universality classes characterized by the new critical exponents, which are shown in table 1 together with those for other three-dimensional universality classes.

Table 1. Critical exponents for the conventional three-dimensional universality classes, and the chiral universality classes, and experimental values for $CsMnBr_3$ and $CsMnI_3$.

	α	β	γ	ν
3D Ising [18]	0.106	0.326	1.238	0.631
3D XY [18]	−0.01	0.345	1.316	0.669
3D Heisenberg [18]	−0.121	0.367	1.388	0.707
Chiral XY [4]	0.34(6)	0.253(10)	1.13(5)	0.54(2)
Chiral Heisenberg [4]	0.24(8)	0.30(2)	1.17(7)	0.59(2)
$CsMnBr_3$	0.40(5) [11]	0.25(1) [12]	1.1(1) [13]	0.53(3) [13]
$CsMnI_3$ (T_{N1})		0.32(1) [20]	1.12(7) [21]	0.59(3) [21]
$CsMnI_3$ (T_{N2})	−0.05(15) [19]	0.35(1) [20]	1.04(3) [21]	0.56(2) [21]

$CsMnBr_3$ and $CsMnI_3$ are typical examples of the stacked TAF with planar and axial anisotropies, respectively. $CsMnBr_3$ undergoes a phase transition at $T_N = 8.3$ K. In the ordered phase, spins lie in the basal plane and form the 120° structure [5,6]. On the other hand, $CsMnI_3$ has two phase transitions at $T_{N1} = 11.2$ K and $T_{N2} = 8.2$ K [7]. In the intermediate phase, the c-axis component of the spin is ordered, with the ferrimagnetic structure in the basal plane. In the low-temperature phase, the perpendicular component of the spin is also ordered, so the spins form a triangular structure including the c-axis, i.e., one-third of the spins are parallel to the c-axis and the rest of the spins are canted from the c-axis [8, 9].

The phase transition of $CsMnBr_3$ has been well investigated from the point of view of criticality by means of neutron scattering experiments and specific heat measurements [10–14]. The critical exponents obtained (see table 1) are in good agreement with the values predicted for the chiral XY universality class. On the other hand, experimental studies of the chiral Heisenberg universality have been scarce, because no suitable model compound without anisotropy is available. The possibility of the experimental study of the universality was pointed out for the weak-anisotropy case, such as that of $CsMnI_3$, under the appropriate magnetic fields [17].

When an external field is applied parallel to the c-axis, $CsMnI_3$ has a multicritical point at which three critical lines of the second-order phase transitions and the first-order spin-flop line meet as shown in figure 1 [15, 16]. Along the $g = 0$ line, where g is a scaling field, the system becomes isotropic in the spin space [17]. Thus, if both temperature and magnetic field (T, H) are varied along the locus $g = 0$, the critical behaviour for the phase transition at the multicritical point should belong to the chiral Heisenberg universality class. In general, however, the locus $g = 0$ is not parallel to the temperature axis. Experimentally, it is difficult to obtain the $g = 0$ line and to vary both T and H maintaining the condition $g = 0$. In order to investigate the critical behaviour belonging to the chiral Heisenberg universality class, we need a TAF without magnetic anisotropy, for which the locus $g = 0$ corresponds to the temperature axis ($H = 0$).

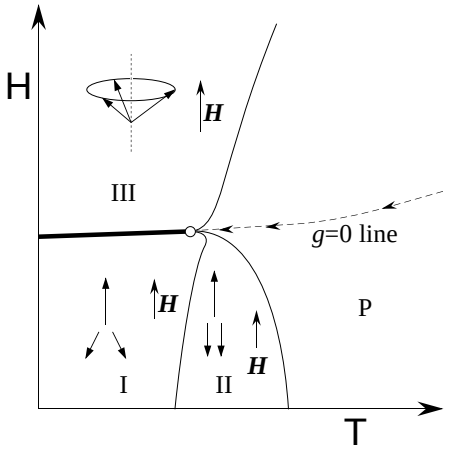

Figure 1. A schematic magnetic phase diagram of $CsMnI_3$. The magnetic field is applied along the c-axis. The thick line (I–III boundary) denotes the first-order spin-flop transition, and the thin curves indicate second-order transition.

Recently, we investigated the phase transition in the triangular antiferromagnetic system $CsMn(Br_xI_{1-x})_3$ by making magnetic susceptibility and torque measurements [23]. Recently, the phase diagram and the critical behaviour of the similar system $CsNi_{0.98}Fe_{0.02}Cl_3$, with planar

anisotropy on average, have been reported by Winkelmann *et al* [22]. In $CsMn(Br_xI_{1-x})_3$, the magnitude and the sign of the anisotropy are systematically controlled by varying the bromine concentration x. Because the present system contains only Mn^{2+} ions as the magnetic ions, the spin state is expected to be homogeneous, which is confirmed by the sharp anomaly in the susceptibility data at the transition temperature. With increasing x, the higher transition temperature T_{N1} decreases in proportion to x, so the intermediate phase becomes narrower and vanishes at $x_c = 0.19$. The anisotropy changes from the axial type to the planar one at $x = x_c$. The result indicates that in $CsMn(Br_{0.19}I_{0.81})_3$ the interaction is almost isotropic on average. Then, we can expect the transition at zero field to belong to the chiral Heisenberg universality class.

In order to investigate the spin structure and the critical behaviour in $CsMn(Br_{0.19}I_{0.81})_3$, we carried out neutron scattering experiments. Here we report the results. The arrangement of this paper is as follows. In section 2, experimental procedures are described. Experimental results and a discussion are given in section 3. The final section is devoted to the conclusions.

2. Experimental procedures

Neutron scattering experiments were performed on the triple-axis spectrometers ISSP-PONTA and HER installed at the research reactor JRR-3M in the Japan Atomic Energy Research Institute (JAERI), Tokai. The spectrometers were used in the double-axis mode to determine the magnetic structure in the ordered state and to observe the critical behaviour. The θ–2θ scans to determine the magnetic structure were mainly carried out on PONTA. For the experiments on the PONTA spectrometer, the experimental conditions were as follows. Pyrolytic graphite (002) reflections were used for the monochromator. To remove higher-order neutrons, a pyrolytic graphite filter was set before the sample. Incident neutron energy was fixed at 14.6 meV. The horizontal collimation sequence was chosen as 15′–10′–10′–open. We could not continue to use the PONTA spectrometer because of limited machine time. Then using the HER spectrometer, we determined the critical exponent for the sublattice magnetization β of $CsMn(Br_{0.19}I_{0.81})_3$. The HER spectrometer was installed at the C1-1 port on the C1 guide tube of the liquid-hydrogen-cooled cold-neutron beam. For the monochromator, pyrolytic graphite (002) reflection was also used. The angular divergence of the beam incident on the monochromator was fixed at 6′. The second, third, and fourth collimators were chosen as 10′, 20′, and open, respectively. Incident neutron energy was fixed at 4.99 meV.

Single crystals of $CsMn(Br_{0.19}I_{0.81})_3$ were prepared by the method described in reference [23]. A single crystal of $CsMn(Br_{0.19}I_{0.81})_3$ with the shape of a triangular prism 5 mm in width and 5 mm in length was used. The sample was mounted in an ILL-type orange cryostat with its [110] and [001] axes in the scattering plane. Sample temperature was measured with a Ge resistance thermometer and was controlled within the accuracy of 0.01–0.001 K.

3. Experimental results

3.1. Magnetic structure

$CsMn(Br_{0.19}I_{0.81})_3$ undergoes a phase transition at $T_N = 8.3$ K [23]. To determine the spin structure of the ordered state, we first measured the integrated intensities of the Bragg reflections observed at $\boldsymbol{q} = (1/3, 1/3, 1)$, (2/3, 2/3, 1), (4/3, 4/3, 1), (5/3, 5/3, 1), (1/3, 1/3, 2), and (2/3, 2/3, 2) at 2 K. These Bragg reflections indicate that the magnetic unit cell in the c-plane is enlarged $\sqrt{3} \times \sqrt{3}$ times. Since the magnetic anisotropy is negligible in the present system, it is considered that spins form the 120° spin structure in the ordered state. When the spin

planes make the angle ϕ with the c-plane as illustrated in figure 2, and they are in multidomain states with respect to the c-axis, the integrated intensity of the magnetic Bragg scattering for $\boldsymbol{q} = (h, h, \ell)$ with $h = n/3$, $\ell \neq 3n$ is given by

$$I \propto \frac{|f(\boldsymbol{q})|}{\sin 2\theta} d^2_{(h,k,\ell)} S^2 \left[\left\{ 2\left(\frac{h}{a}\right)^2 + \left(\frac{\ell}{c}\right)^2 \right\} (1 + \cos^2\phi) + \left(\frac{2h}{a}\right)^2 \sin^2\phi \right] \tag{1}$$

and $I = 0$ for integer h, where 2θ is the scattering angle, $f(\boldsymbol{q})$ is the magnetic form factor, $d_{(h,k,\ell)}$ is the spacing of the (h, k, ℓ) lattice plane, and a and c are lattice constants. For $f(\boldsymbol{q})$, we used the spherical magnetic form factors calculated by Watson and Freeman [24]. The lattice constants a and c are determined from the (110) and (002) nuclear reflections. Minimizing the reliability factor R given by

$$R = \sum_{h,k,\ell} |I_{\mathrm{calc}}(h, k, \ell) - I_{\mathrm{obs}}(h, k, \ell)| \Big/ \sum_{h,k,\ell} I_{\mathrm{obs}}(h, k, \ell)$$

we obtain $\langle \cos^2\phi \rangle = 0.362$, i.e., $\langle \phi \rangle = 53^\circ$, where $\langle \cdots \rangle$ denotes the spatial average. In table 2, we show the experimental and calculated intensities of several Bragg reflections together with the calculated intensities for $\phi = 0^\circ$ and 90°. In table 2, the Bragg intensities are normalized to that of the (1/3, 1/3, 1) reflection. The spin structures for $\phi = 0^\circ$ and 90° correspond to those of $CsMnBr_3$ and $CsMnI_3$. We see from table 2 that the spins form the 120° structure neither in the c-plane nor along the c-axis, but in the plane making an angle of 53° with the c-plane on average.

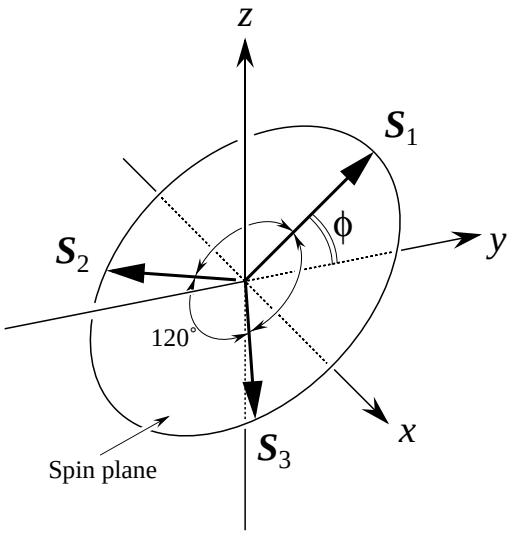

Figure 2. The spin structure in the ordered state. The angle ϕ denotes the angle between the spin plane and the c-plane. The x- and y-axis are taken in the c-plane.

When the directions of the spin planes have the isotropic distribution, the average of $\cos^2\phi$ is given by $\langle \cos^2\phi \rangle = 1/3$, which leads to $\langle \phi \rangle = 55^\circ$. This angle is very close to $\langle \phi \rangle = 53^\circ$ obtained by minimizing the R-factor. Thus we can interpret the experimental results as indicating that the spin planes are almost isotropically distributed in the present system. This is consistent with the fact that the anisotropy is nearly negligible.

Table 2. Experimental and calculated intensities of several magnetic Bragg reflections in $CsMn(I_{0.81}Br_{0.19})_3$. They are normalized to (1/3, 1/3, 1) reflections. The calculated intensities for $\phi = 0^\circ$ and 90° are also shown for comparison.

(h, k, ℓ)	$I_{obs}(T = 2\ K)$	$I_{calc}(\langle\cos^2\phi\rangle = 0.362)$	$I_{calc}(\phi = 0^\circ)$	$I_{calc}(\phi = 90^\circ)$
$(\frac{1}{3}, \frac{1}{3}, 1)$	1	1	1	1
$(\frac{2}{3}, \frac{2}{3}, 1)$	0.678	0.691	0.573	0.797
$(\frac{4}{3}, \frac{4}{3}, 1)$	0.298	0.296	0.200	0.383
$(\frac{5}{3}, \frac{5}{3}, 1)$	0.210	0.190	0.123	0.250
$(\frac{1}{3}, \frac{1}{3}, 3)$	0.178	0.178	0.197	0.161
$(\frac{2}{3}, \frac{2}{3}, 3)$	0.144	0.125	0.132	0.118
		$R = 2.15\%$	$R = 12.8\%$	$R = 11.4\%$

3.2. Critical behaviour

The magnetic Bragg intensity I_{Bragg} is proportional to the square of the sublattice magnetization. In the critical region below T_N, I_{Bragg} is described as

$$I_{Bragg} \propto \left(\frac{T_N - T}{T_N}\right)^{2\beta} \tag{2}$$

where β is the critical exponent of the sublattice magnetization.

For strict correction of the background and critical scattering, the scan along the $(h, h, 1)$ direction was performed. An example of the scan performed at $T = 8.266(1)$ K ($T < T_N$) is shown in figure 3. The data have not been convoluted with the resolution function. The profiles obtained around (1/3, 1/3, 1) at different temperatures were fitted to the following form:

$I_{obs}(h, k, \ell) =$ magnetic Bragg scattering with Gaussian shape
+ diffuse signal with Lorentzian shape
+ background.

Figure 4 shows a log–log plot of the magnetic Bragg peak intensity for $\boldsymbol{q} = (1/3, 1/3, 1)$ versus reduced temperature $(T_N - T)/T_N$ with $T_N = 8.291(1)$ K, which is determined simultaneously with β. Fitting equation (2) to the experimental data over the range $0.005 < (T_N - T)/T_N < 0.1$, we obtain $\beta = 0.28 \pm 0.02$. This value agrees with the value $\beta = 0.30 \pm 0.02$ predicted for the chiral Heisenberg universality class [4].

For a more decisive experiment, measurement of the critical exponent α for the specific heat is desired, because the exponent $\alpha = 0.24 \pm 0.08$ predicted for the chiral Heisenberg universality class differs significantly from those of the conventional three-dimensional ($\alpha \simeq -0.121$) and chiral XY ($\alpha = 0.34 \pm 0.06$) universality classes.

4. Conclusions

We have presented the results of elastic neutron scattering experiments on a triangular antiferromagnet, $CsMn(Br_{0.19}I_{0.81})_3$, for which our previous magnetic measurements revealed the magnetic anisotropy to be negligible. In the ordered state below $T_N = 8.29$ K, the spin planes in which the spins lie with the 120° structure are tilted from the basal plane, and the average of the tilting angle ϕ is evaluated as $\langle\cos^2\phi\rangle = 0.362$, i.e., $\langle\phi\rangle = 53^\circ$. This result suggests that the spin planes have almost isotropic distribution.

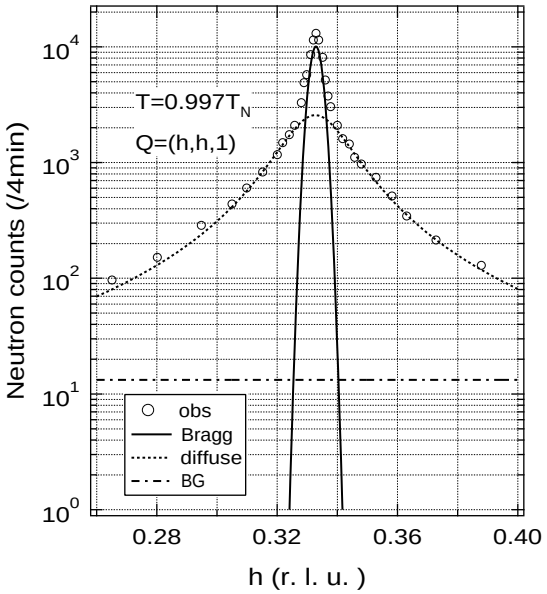

Figure 3. An example of a scan along the $(h, h, 1)$ line around the (1/3, 1/3, 1) reflection on a logarithmic scale. Solid and dashed curves and the dot–dashed line indicate the magnetic Bragg scattering, diffuse scattering, and background, respectively.

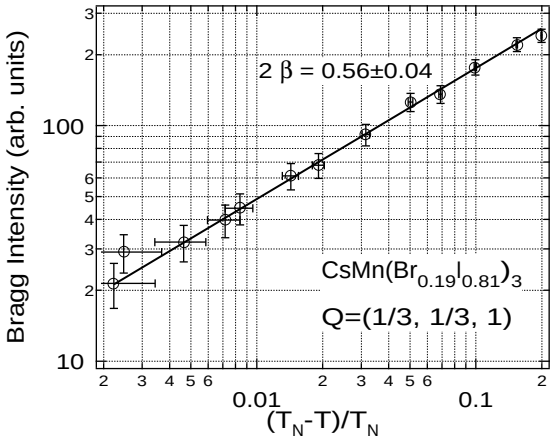

Figure 4. A log–log plot of the magnetic Bragg peak intensity $I_{\rm Bragg}$ versus reduced temperature $(T_{\rm N} - T)/T_{\rm N}$ for the $Q = (1/3, 1/3, 1)$ reflection. The solid line is a fit to the power law $I_{\rm Bragg} \propto (1 - T/T_{\rm N})^{2\beta}$, with $2\beta = 0.56 \pm 0.04$ and $T_{\rm N} = 8.291(1)$ K.

The critical exponent β for the sublattice magnetization is obtained as $\beta = 0.28 \pm 0.02$, which agrees with the predicted one for the chiral Heisenberg universality class.

References

[1] Collins M F and Petrenko O A 1997 *Can. J. Phys.* **75** 605
[2] Miyashita S and Shiba H 1984 *J. Phys. Soc. Japan* **53** 1145

[3] Lee D H, Joannopoulos J D, Negele J W and Landau D P 1986 *Phys. Rev.* B **33** 450
[4] Kawamura H 1992 *J. Phys. Soc. Japan* **61** 1299
Kawamura H 1998 *J. Phys.: Condens. Matter* **10** 4707
[5] Eibschütz M, Sherwood R C, Hsu F S L and Cox D E 1972 *AIP Conf. Proc.* 864
[6] Falk U, Furrer A, Güdel H U and Kjems J K 1987 *Phys. Rev.* B **35** 4888
[7] Iio K, Hotta H, Sano M, Masuda H, Tanaka H and Nagata K 1988 *J. Phys. Soc. Japan* **57** 50
[8] Zandbergen H W 1980 *J. Solid State Chem.* **35** 367
[9] Harrison A, Collins M F, Abu-Dayyeh J and Stager C V 1991 *Phys. Rev.* B **43** 679
[10] Mason T E, Gaulin B D and Collins M F 1989 *Phys. Rev.* B **39** 586
[11] Deutshmann R, von Löhneysen H, Wosnitza J, Kremer R K and Visser D 1992 *Europhys. Lett.* **17** 637
[12] Ajiro Y, Nakashima T, Unno Y, Kadowaki H, Mekata M and Achiwa N 1988 *J. Phys. Soc. Japan* **57** 2648
[13] Kadowaki H, Shapiro S M, Inami T and Ajiro Y 1988 *J. Phys. Soc. Japan* **57** 2640
[14] Weber H, Beckmann D, Wosnitza J, von Löhneysen H and Visser D 1995 *Int. J. Mod. Phys.* B **9** 1387
[15] Katori H A, Goto T and Ajiro Y 1993 *J. Phys. Soc. Japan* **62** 743
[16] Enderle M, Furtuna G and Steiner M 1994 *J. Phys.: Condens. Matter* **6** L385
[17] Kawamura H, Caillé A and Plumer M L 1990 *Phys. Rev.* B **41** 4416
[18] Collins M F 1989 *Magnetic Critical Scattering* (New York: Oxford University Press) p 29
[19] Beckmann D, Wosnitza J, von Löhneysen H and Visser D 1993 *J. Phys.: Condens. Matter* **5** 6289
[20] Ajiro Y, Inami T and Kadowaki H 1990 *J. Phys. Soc. Japan* **59** 4142
[21] Kadowaki H, Inami T, Ajiro Y, Nakajima K and Endoh Y 1991 *J. Phys. Soc. Japan* **60** 1708
[22] Winkelmann M, Schneider R, Enderle M, Asano T, Ajiro Y and Steiner M 1997 *J. Phys.: Condens. Matter* **9** 703
[23] Ono T, Tanaka H, Kato T and Iio K 1998 *J. Phys.: Condens. Matter* **10** 7209
[24] Watson R E and Freeman A J 1961 *Acta Crystallogr.* **14** 27